Hindawi Publishing Corporation
Journal of Nanomaterials
Volume 2014, Article ID 186916, 7 pages
http://dx.doi.org/10.1155/2014/186916

Review Article

ZnO Film Photocatalysts

Bosi Yin,[1] Siwen Zhang,[1] Dawei Zhang,[2] Yang Jiao,[1] Yang Liu,[1] Fengyu Qu,[1] and Xiang Wu[1]

[1] *Key Laboratory for Photonic and Electronic Bandgap Materials, Ministry of Education, Harbin Normal University, Harbin 150025, China*
[2] *College of Life Science and Technology, Harbin Normal University, Harbin 150025, China*

Correspondence should be addressed to Xiang Wu; wuxiang05@gmail.com

Received 27 December 2013; Accepted 4 January 2014; Published 17 March 2014

Academic Editor: Chuanfei Guo

We have synthesized high-quality, nanoscale ultrathin ZnO films at relatively low temperature using a facile and effective hydrothermal approach. ZnO films were characterized by scanning electron microscope (SEM), X-ray diffraction (XRD), Raman spectroscopy, photoluminescence spectra (PL), and UV-vis absorption spectroscopy. The products demonstrated 95% photodegradation efficiency with Congo red (CR) after 40 min irradiation. The photocatalytic degradation experiments of methyl orange (MO) and eosin red also were carried out. The results indicate that the as-obtained ZnO films might be promising candidates as the excellent photocatalysts for elimination of waste water.

1. Introduction

Zinc oxide (ZnO), an important II-VI semiconductor with a bandgap energy of 3.37 eV and a large exciton binding energy of 60 meV at room temperature, has been extensively studied because of its potential applications in solar cells [1], sensors [2, 3], photocatalysis [4], and so forth. Among them, the important application of ZnO as a photocatalyst in environmental protection cannot be ignored [5–10]. In the past decades, zero-dimensional (0D) and one-dimensional (1D) ZnO nanostructures have been extensively studied with the aims of developing novel applications [11–25]. However, two-dimensional (2D) nanostructures have not been extensively explored [26, 27]. Since the photocatalytic reaction occurs at surface of the materials, the nanosized semiconductor will increase the decomposition rate because of the increased surface area. Therefore, the synthesis of novel ZnO nanostructure that is stable against aggregation and possesses a higher surface-to-volume ratio is still an important task for its environmental remediation applications. In the fabrication of 2D ZnO nanostructures, previous methods required either multiple operation steps [28, 29] or using of the templates or the toxic reactants [30, 31]. Therefore, developing a simple and efficient green method to synthesize ZnO films will be highly required.

Herein, we used a facile hydrothermal approach to obtain ultrathin ZnO films without using any surfactants or templates. Such ZnO film structures exhibit a significantly improved photocatalytic activity in the photodegradation of MO than that of other structured ZnO. This work provides a way to improve the photocatalytic performance by designing a desirable nanoarchitecture.

2. Experimental Details

All reagents were of analytical grade and were used without further purification. In a typical procedure, 20 mL of Zn $(NO_3)_2$ solution was added to 20 mL urea aqueous solution. After a continuous stirring for 30 min, the mixed solution was transferred into a 100 mL stainless steel autoclave, which was sealed subsequently and kept at 150°C for 3 h. The white precipitation was centrifugated and washed several times with deionized water, followed by drying in air at 60°C for 8 h.

The morphology and microstructures of the as-obtained products were characterized by scanning electron microscope (SEM; Hitachi S-4800), XRD (D/max2600, Rigaku), and Raman spectroscope (HR800). Photoluminescence spectra (PL) of the samples were characterized by the micro-Raman spectrometer (HR800) under the excitation

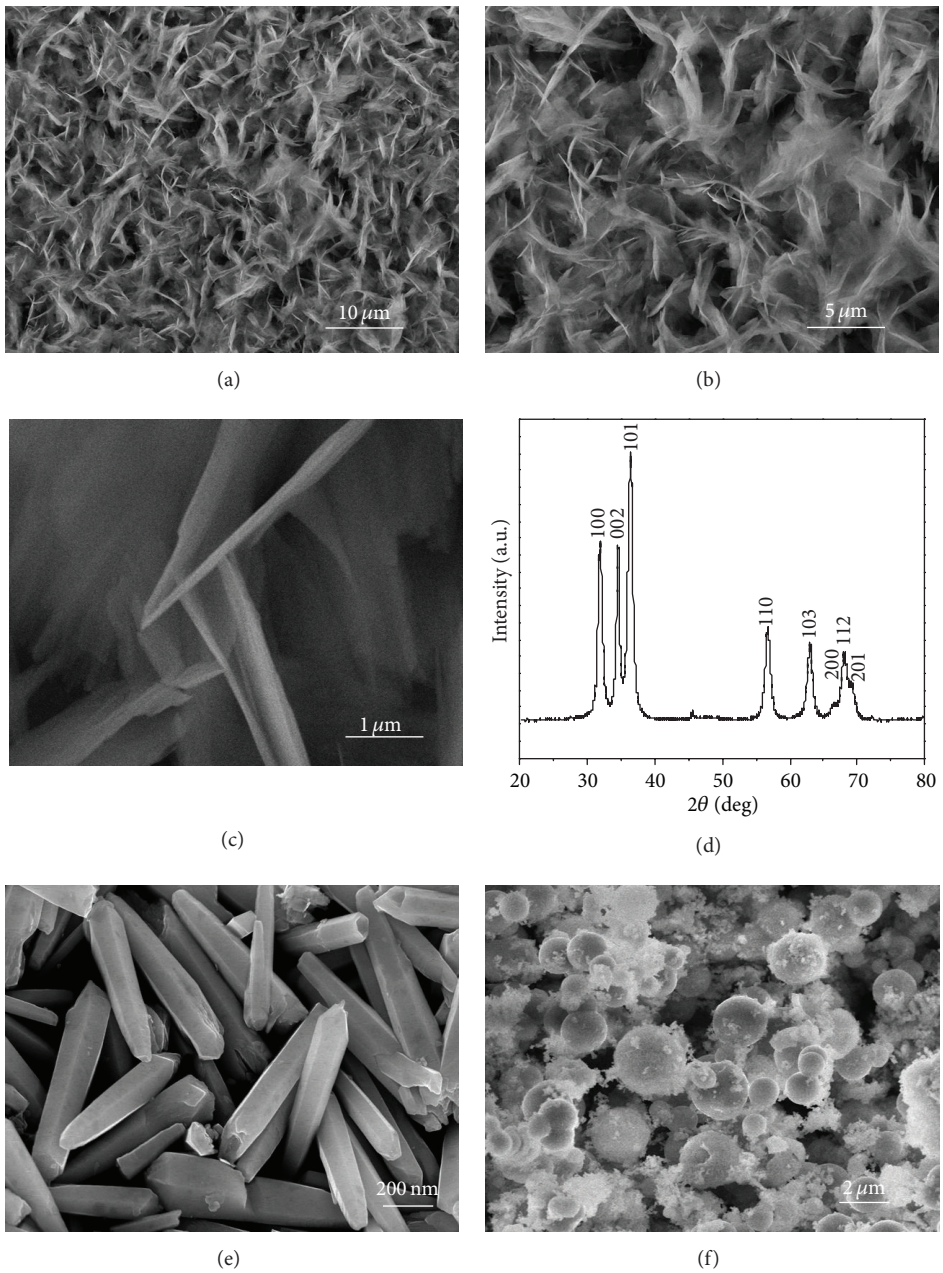

Figure 1: (a–c) SEM images of the as-synthesized ZnO films at different magnification. (d) XRD pattern of as-synthesized ZnO products. (e) SEM images of ZnO nanocones. (f) SEM images of ZnO commercial powder.

wavelength of 325 nm. The efficiency of the photocatalytic degradation was analyzed by monitoring dye decolorization at the maximum absorption wavelength, using a UV-vis spectrometer (Shimadzu UV-2550).

The photocatalytic experiment of the as-synthesized ZnO samples for decomposing MO was conducted as follows: 0.1 g ZnO films were suspended in 200 mL MO aqueous solution (20 mg L^{-1}). The solution was continuously stirred for 1 h in the dark to ensure the establishment of an adsorption-desorption equilibrium between ZnO film and MO. Then the solution was exposed to UV irradiation from a 500 W Hg lamp at room temperature. The samples were collected at regular interval to measure MO degradation by UV-vis spectra. The products were then separated from the solution by centrifuging, washed with ethanol to fully remove the residual organic species then with water, and reused for the next run. Finally, the experiments of the photocatalytic degradation of CR aqueous solution and eosin red aqueous solution also were conducted under the same conditions.

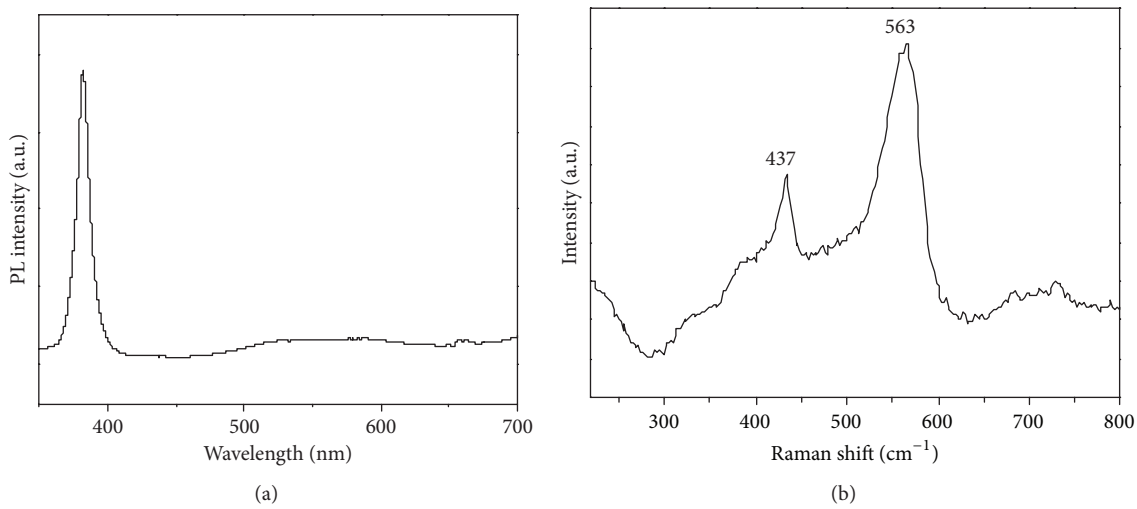

Figure 2: (a) PL spectra of the synthesized product. (b) Raman spectrum of the synthesized product.

3. Results and Discussion

The general morphology of ZnO products was investigated by SEM. Figures 1(a)–1(c) show the SEM images of the as-synthesized ZnO products at different magnifications, finding that the as-obtained product consists of a layer of film with an average thickness of 30 nm. XRD pattern for ZnO film is shown in Figure 1(d). All of the diffraction peaks can be well indexed to hexagonal wurtzite ZnO (JCPDS number 36-1451) with lattice constants of $a = b = 3.25$ Å and $c = 5.2$ Å. No diffraction peaks from any other impurities are identified, indicating high purity of the product. To further investigate the structures of the ZnO films, PL spectra of the product were conducted. Figures 1(e) and 1(f) are SEM images of ZnO nanocones and ZnO commercial powder, respectively.

Figure 2(a) showed a strong ultraviolet emission peak and a weak green light emission. It is known that the UV peak arises from the near band-edge exciton recombination, and the green emission comes from the various defect states. Figure 2(b) presents Raman spectrum of the as-obtained product at room temperature. Two peaks are observed at 437 and 563 cm^{-1}, respectively. ZnO with wurtzite structure belongs to the C_{6v} space group with the two formula units per primitive cell and all the atoms occupy the C_{3v} symmetry. Near the center of the Brillouin zone, the group theory predicts the existence of the different optical modes. Raman active modes for wurtzite ZnO are $\Gamma = A_1 + 2E_2 + E_1$, where the A_1, E_1, and $2E_2$ modes are Raman active and split into longitudinal (LO) and transverse (TO) optical modes [32, 33]. The peak at 437 cm^{-1} in Figure 2(b) is assigned to E_2 optical phonon which corresponds to the band characteristic of ZnO wurtzite hexagonal phase [34]. Peaks located at 563 cm^{-1} correspond to the LO phonon of A_1 and longitudinal E_1, respectively.

In order to investigate the photocatalytic efficiency of ZnO structures with different morphologies, we examined the decomposition of MO in water under irradiation of a 500 W Hg lamp as the light source. For comparison, decomposition of ZnO nanocones and that of commercial powder were also conducted under the same experimental condition. Figure 3(a) shows the adsorption spectra of MO solution in the presence of ZnO films under Hg lamp light. The absorption peak corresponding to MO at 465 nm diminished gradually and the photocatalytic degradation rate of MO is 96% after 90 min. The adsorption spectra of MO solution in the presence of ZnO nanocones are shown in Figure 3(b), revealing its photocatalytic degradation rate of 73%. For commercial powder, the degradation rate is 84% (seen in Figure 3(c)). Figure 3(d) shows the curves of the degradation rate of MO solution for blank experiment (black curve), ZnO films (pink curve), ZnO nanocones (red curve), and commercial powder (blue curve). Experimental results show that the degradation rate of MO in the presence of ZnO films is the fastest. The superior photocatalytic activities of ZnO films may arise from their unique structures and surface reaction sites. Specifically, ZnO films possess several outstanding features, such as the large surface volume ratio, the effective electron-hole separation of the Schottky barriers, and thin thickness. It might be that higher surface area increases the number of active sites and promotes separation efficiency of the electron-hole pairs, resulting in the improvement of photocatalytic activity. And the separation and mobility of the electron-hole pairs were intensely suppressed in wide band gap. Hence, ZnO films can absorb and transport more dye molecules on their surface.

Finally, the photocatalytic activities of the as-synthesized ZnO films for the degradation of different organic pollutants (MO, eosin red, and CR) were carried out. Figure 4(a) shows the adsorption spectra of MO solution in the presence of ZnO films under ultraviolet light at different intervals of time. Figure 4(b) shows the adsorption spectra of eosin red solution. The main absorption peak is centered at 517 nm before and after irradiation. When the illumination time was extended to 60 min, the absorption peak diminished

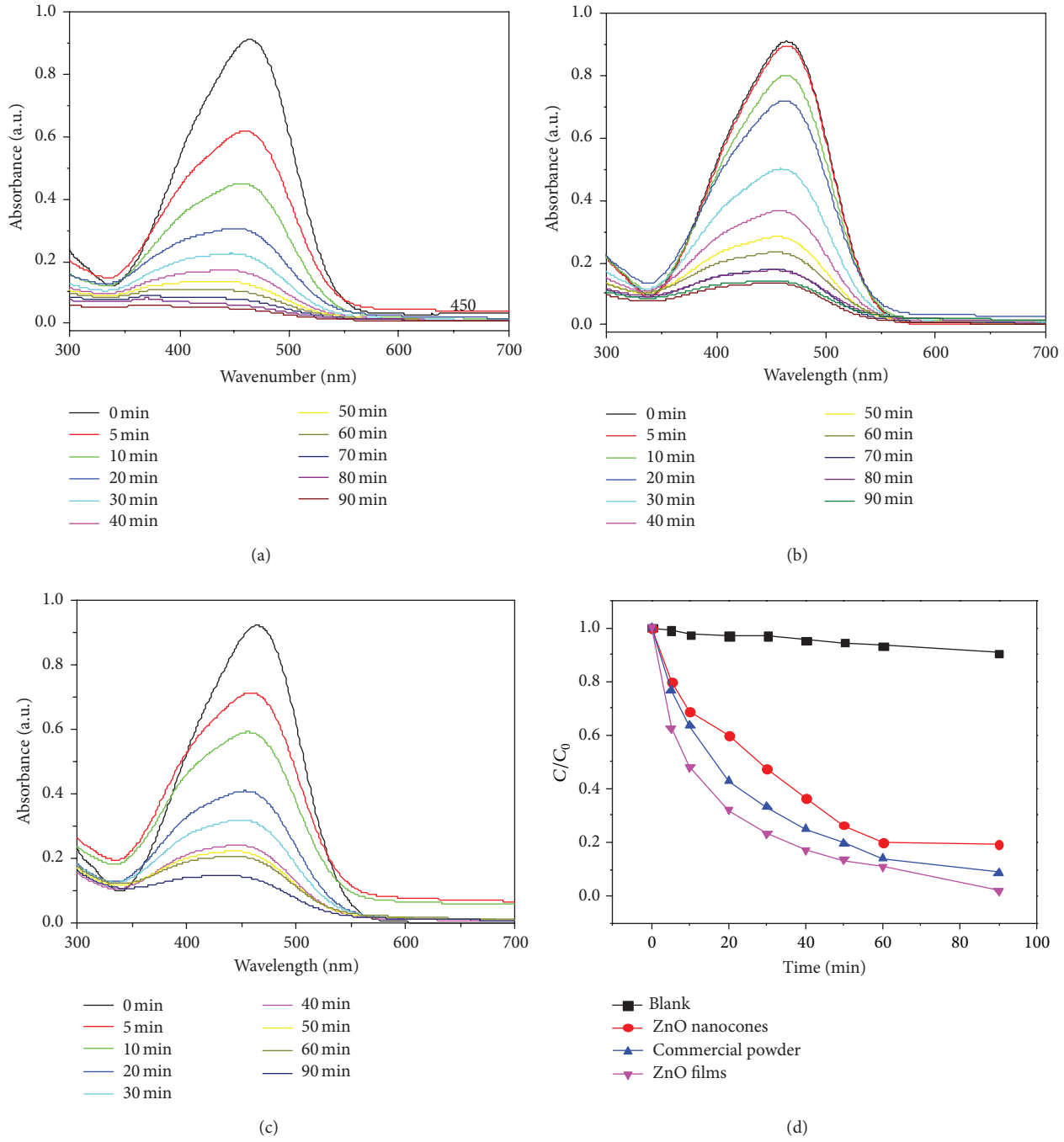

FIGURE 3: Adsorption spectra of MO solution in the presence of different ZnO nanostructures. (a) ZnO films. (b) ZnO nanocones. (c) ZnO commercial powder. (d) Degradation rate curve of ZnO films, ZnO nanocones, and ZnO commercial powder.

gradually and the photodegradation ratio of eosin red was up to 98%. Figure 4(c) shows the adsorption spectra of CR with the absorption peak of 495 nm. Nearly 95% of CR dye molecules were decomposed in 40 min. In order to illustrate for which dyes ZnO film are highly selective, we take the same 40 min to compare the degradation efficiency of different dyes according to Figures 4(a)–4(c). The changes of the organic pollutants concentration under visible irradiation can be calculated as follows:

$$I = \frac{C}{C_0} \times 100\%, \quad (1)$$

where C_0 is the initial concentration of the organic pollutants when the ultraviolet light is turned on, while the real time

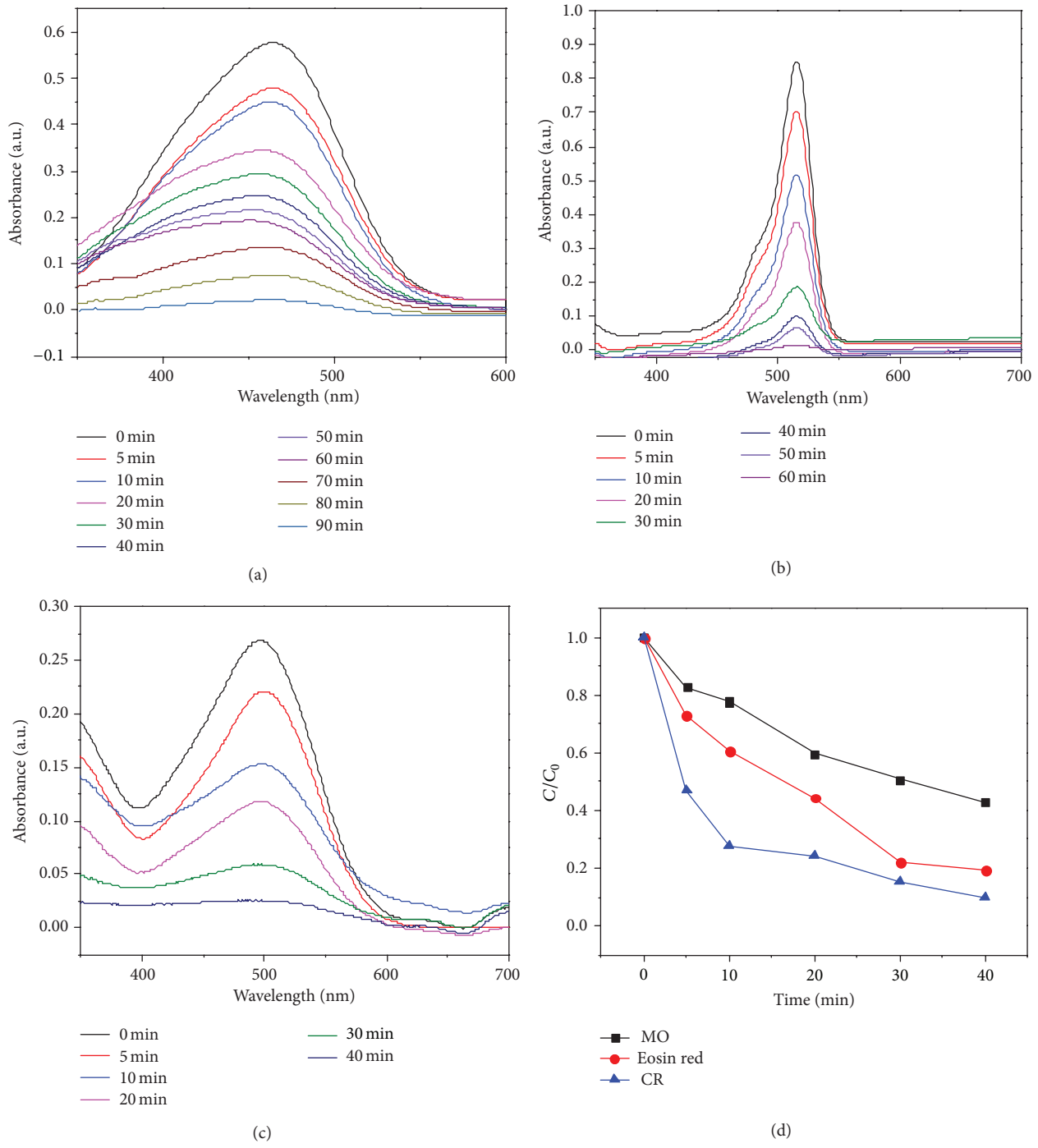

FIGURE 4: Variations of adsorption spectra of the organics dye solution in the presence of ZnO films irradiated by a Hg lamp for different time; (a) MO, (b) eosin red, and (c) CR (d); photocatalysis degradation rate of MO, eosin red, and CR.

concentration of organic pollutants under the ultraviolet light irradiation is expressed by C. Photocatalytic efficiency derived from the changes of the organic dyes concentration can be represented by the relative ratio C/C_0. The order of degradation rate was MO (58%) < eosin red (88%) < CR (95%), as shown in Figure 4(d). It show that ZnO films possess the highest degradation efficiency to CR solution than to the others.

4. Conclusions

In summary, ultrathin ZnO films have been successfully synthesized by a simple hydrothermal approach without any surfactants or templates. The as-obtained films possess the average thickness of 30 nm. The photocatalytic experiments revealed that ZnO films possess the highest photocatalytic activity for the degradation of CR dye under ultraviolet

light irradiation. And the degradation rate is 95% in 40 min. It is expected that such ZnO films could have potential application in eliminating organic pollutant in wastewater.

Conflict of Interests

The authors declare that they have no conflict of interests regarding the publication of this paper.

Authors' Contribution

Bosi Yin and Siwen Zhang contributed equally to this work.

Acknowledgments

This work was supported by the Foundation for Key Project of Ministry of Education (no. 211046), China, Program for New Century Excellent Talents in Heilongjiang Provincial University (1252-NCET-018), the Scientific Research Fund of Heilongjiang Provincial Education Department (12531179), and Program for Scientific and Technological Innovation Team Construction in Universities of Heilongjiang (no. 2011TD010).

References

[1] K. Hara, T. Horiguchi, T. Kinoshita, K. Sayama, H. Sugihara, and H. Arakawa, "Highly efficient photon-to-electron conversion with mercurochrome-sensitized nanoporous oxide semiconductor solar cells," *Solar Energy Materials and Solar Cells*, vol. 64, no. 2, pp. 115–134, 2000.

[2] S. Zhuiykov, V. Plashnitsa, and N. Miura, "Effect of ZnO doping on morphology and electrochemical properties of sub-micron RuO_2 sensing electrode of DO sensor," *Materials Letters*, vol. 65, no. 6, pp. 991–994, 2011.

[3] S. Zhuiykov and E. Kats, "Influence of sintering temperatures on the performance of ZnO-doped RuO_2 sensing electrode of electrochemical DO sensor," *Materials Science and Engineering Division*, vol. 104, pp. 592–595, 2000.

[4] B. X. Jia, W. N. Jia, X. Wu, and F. Y. Qu, "Hierarchical porous SnO_2 microflowers photocatalyst," *Science of Advanced Materials*, vol. 4, pp. 1127–1133, 2012.

[5] B. X. Jia, W. N. Jia, Y. L. Ma, X. Wu, and F. Y. Qu, "SnO_2 core-shell microspheres with excellent photocatalytic properties," *Science of Advanced Materials*, vol. 4, pp. 702–707, 2012.

[6] W. N. Jia, X. Wu, B. X. Jia, F. Y. Qu, and H. J. Fan, "Self assembled porous ZnS nanospheres with high photocatalytic performance," *Science of Advanced Materials*, vol. 5, pp. 1329–1336, 2013.

[7] H. Yumoto, T. Inoue, S. J. Li, T. Sako, and K. Nishiyama, "Application of ITO films to photocatalysis," *Thin Solid Films*, vol. 345, no. 1, pp. 38–41, 1999.

[8] J. Wang, F. Y. Qu, and X. Wu, "Synthesis of ultra-thin ZnO nanosheets: photocatalytic and superhydrophilic properties," *Science of Advanced Materials*, vol. 5, pp. 1052–1059, 2013.

[9] B. X. Jia, W. N. Jia, F. Y. Qu, and X. Wu, "General strategy for self assembly of mesoporous SnO_2 nanospheres and their applications in water purification," *RSC Advances*, vol. 3, pp. 12140–12148, 2013.

[10] J. Wang, F. Y. Qu, and X. Wu, "Photocatalytic degradation of organic dyes with hierarchical Ag_2O/ZnO heterostructures," *Science of Advanced Materials*, vol. 5, pp. 1364–1371, 2013.

[11] K. Sato, M. Hyodo, J. Takagi, M. Aoki, and R. Noyori, "Hydrogen peroxide oxidation of aldehydes to carboxylic acids: an organic solvent-, halide- and metal-free procedure," *Tetrahedron Letters*, vol. 41, no. 9, pp. 1439–1442, 2000.

[12] J. Wang, F. Y. Qu, and X. Wu, "High selective photocatalytic properties of three dimensional hierarchical ZnO microflowers," *Materials Express*, vol. 3, pp. 256–264, 2013.

[13] A. J. Hoffman, E. R. Carraway, and M. R. Hoffmann, "Photocatalytic production of H_2O_2 and organic peroxides on quantum- sized semiconductor colloids," *Environmental Science and Technology*, vol. 28, no. 5, pp. 776–785, 1994.

[14] Y. Liu, Y. Jiao, B. S. Yin, S. W. Zhang, F. Y. Qu, and X. Wu, "Hierarchical semiconductor oxide photocatalyst: a case of the SnO_2 microflower," *Nano-Micro Letters*, vol. 5, pp. 234–241, 2013.

[15] S. T. Christoskova and M. Stoyanova, "Catalytic degradation of CH_2O and $C_6H_5CH_2OH$ in wastewaters," *Water Research*, vol. 36, no. 9, pp. 2297–2303, 2002.

[16] K. Gupta, S. Bhattacharya, D. Chattopadhyay et al., "Ceria associated manganese oxide nanoparticles: synthesis, characterization and arsenic(V) sorption behavior," *Chemical Engineering Journal*, vol. 172, no. 1, pp. 219–229, 2011.

[17] T. Ozkaya, A. Baykal, H. Kavas, Y. Köseoğlu, and M. S. Toprak, "A novel synthetic route to Mn_3O_4 nanoparticles and their magnetic evaluation," *Physica B: Condensed Matter*, vol. 403, no. 19-20, pp. 3760–3764, 2008.

[18] K. A. M. Ahmed, H. Peng, K. Wu, and K. Huang, "Hydrothermal preparation of nanostructured manganese oxides (MnOx) and their electrochemical and photocatalytic properties," *Chemical Engineering Journal*, vol. 172, no. 1, pp. 531–539, 2011.

[19] Y. X. Wang, X. Y. Li, G. Lu, X. Quan, and G. Chen, "Highly oriented 1-D ZnO nanorod arrays on zinc foil: direct growth from substrate, optical properties and photocatalytic activities," *Journal of Physical Chemistry C*, vol. 112, no. 19, pp. 7332–7336, 2008.

[20] Y. Chen, Z. Duan, Y. Min, M. Shao, and Y. Zhao, "Synthesis, characterization and catalytic property of manganese dioxide with different structures," *Journal of Materials Science: Materials in Electronics*, vol. 22, no. 8, pp. 1162–1167, 2011.

[21] J. Luo, H. T. Zhu, H. M. Fan et al., "Synthesis of single-crystal tetragonal α-MnO_2 nanotubes," *Journal of Physical Chemistry C*, vol. 112, no. 33, pp. 12594–12598, 2008.

[22] M. Zhou, X. Zhang, J. Wei, S. Zhao, L. Wang, and B. Feng, "Morphology-controlled synthesis and novel microwave absorption properties of hollow urchinlike α-MnO_2 nanostructures," *Journal of Physical Chemistry C*, vol. 115, no. 5, pp. 1398–1402, 2011.

[23] C. Borchers, S. Müller, D. Stichtenoth, D. Schwen, and C. Ronning, "Catalyst-nanostructure interaction in the growth of 1-D ZnO nanostructures," *Journal of Physical Chemistry B*, vol. 110, no. 4, pp. 1656–1660, 2006.

[24] H. J. Zhou and S. S. Wong, "A facile and mild synthesis of 1-D ZnO, CuO, and α-Fe_2O_3 nanostructures and nanostructured arrays," *ACS Nano*, vol. 2, no. 5, pp. 944–958, 2008.

[25] J. Cao, Y. Zhu, K. Bao, L. Shi, S. Liu, and Y. Qian, "Microscale Mn_2O_3 hollow structures: sphere, cube, ellipsoid, dumbbell, and their phenol adsorption properties," *Journal of Physical Chemistry C*, vol. 113, no. 41, pp. 17755–17760, 2009.

[26] C. F. Guo, S. Cao, J. Zhang et al., "Topotactic transformations of superstructures: from thin films to two-dimensional networks to nested two-dimensional networks," *Journal of the American Chemical Society*, vol. 133, no. 21, pp. 8211–8215, 2011.

[27] C. F. Guo, J. M. Zhang, Y. Tian, and Q. Liu, "A general strategy to superstructured networks and nested self-similar networks of bismuth compounds," *ACS Nano*, vol. 6, pp. 8746–8752, 2012.

[28] H. Zhang, R. Wu, Z. Chen, G. Liu, Z. Zhang, and Z. Jiao, "Self-assembly fabrication of 3D flower-like ZnO hierarchical nanostructures and their gas sensing properties," *CrystEngComm*, vol. 14, no. 5, pp. 1775–1782, 2012.

[29] A. Sinhamahapatra, A. K. Giri, P. P. Pahari, and S. K. Bajaj, "A rapid and green synthetic approach for hierarchically assembled porous ZnO nanoflakes with enhanced catalytic activity," *Journal of Materials Chemistry*, vol. 22, pp. 17227–17235, 2012.

[30] F. Lu, W. Cai, and Y. Zhang, "ZnO hierarchical micro/nano-architectures: solvothermal synthesis and structurally enhanced photocatalytic performance," *Advanced Functional Materials*, vol. 18, no. 7, pp. 1047–1056, 2008.

[31] H. Fan and X. Jia, "Selective detection of acetone and gasoline by temperature modulation in zinc oxide nanosheets sensors," *Solid State Ionics*, vol. 192, no. 1, pp. 688–692, 2011.

[32] X. Wu, P. Jiang, W. Cai, X.-D. Bai, P. Gao, and S.-S. Xie, "Hierarchical ZnO micro-/nano-structure film," *Advanced Engineering Materials*, vol. 10, no. 5, pp. 476–481, 2008.

[33] A. Umar, S. H. Kim, Y.-S. Lee, K. S. Nahm, and Y. B. Hahn, "Catalyst-free large-quantity synthesis of ZnO nanorods by a vapor-solid growth mechanism: structural and optical properties," *Journal of Crystal Growth*, vol. 282, no. 1-2, pp. 131–136, 2005.

[34] T. C. Damen, S. P. S. Porto, and B. Tell, "Raman effect in zinc oxide," *Physical Review*, vol. 142, no. 2, pp. 570–574, 1966.